Ceramics International 44 (2018) 4653–4659

Contents lists available at ScienceDirect

Ceramics International

journal homepage: www.elsevier.com/locate/ceramint

Residual stress control in CrAlN coatings deposited on Ti alloys

Yanyun Bai[a], Yeting Xi[a], Kewei Gao[a], Huisheng Yang[a], Xiaolu Pang[a,*], Alex A. Volinsky[b]

[a] School of Materials Science and Engineering, University of Science and Technology Beijing, No. 30 Xueyuan Road, Haidian District, Beijing 100083, China
[b] Department of Mechanical Engineering, University of South Florida, Tampa, FL 33620, USA

ARTICLE INFO

Keywords:
CrAlN coatings
Interlayer
Crystal microstructure
Residual stress
Mechanical properties

ABSTRACT

In order to control residual stress of CrAlN coatings on Ti substrates, ~70 nm CrAl interlayer was deposited at different temperatures. Residual stress and coatings' structure were characterized by X-ray diffraction. Residual stress in the coatings was compressive and increased with CrAl interlayer deposition temperature. Residual stress in 1.5 μm, 2 μm and 2.6 μm thick CrAlN films on TC21 with the interlayer deposited at 100 °C (−47.43 MPa, −25.57 MPa and −855.77 MPa, respectively) was smaller than with the interlayer deposited at 300 °C (−1.39 GPa, −1.95 GPa and −1.62 GPa, respectively). The coatings on the TC4 substrate showed the same trend (−1.02 GPa, −389.91 MPa and −1.03 GPa for the interlayer deposited at 100 °C, respectively, and −921.42 MPa, −2.31 GPa and −1.80 GPa for the interlayer deposited at 100 °C, respectively). Changing the interlayer deposition temperature can influence the coatings' residual stress and crystal structure, and improve mechanical properties of the coatings. CrAlN deposition is a convenient and efficient way to improve mechanical properties of Ti alloys.

1. Introduction

Due to low density, good mechanical properties and biocompatibility, titanium alloys have been widely used in aerospace, military and medical applications. However, poor wear resistance has been the main barrier for Ti alloys applications as structural materials [1–3]. Various efforts have been made to improve tribological properties of Ti alloys [1,2,4–8]. Surface modification is one of the methods to improve the surface quality of Ti alloys. Previous reports have shown that surface treatment, such as plasma nitriding, has positive effects on subsequent coatings deposition, along with improved wear resistance [9–13]. Farokhzadeh and Edrisy studied 600 °C plasma nitriding treatment of the Ti-6Al-4V alloy, and demonstrated 552 MPa endurance limit, which was higher compared with conventional 750–1100 °C nitriding [14]. Fan et al. proposed vacuum braze coating process to prepare ultra-hard thick composite coatings on titanium alloys, and fabricated intermetallic composite coating using ceramic additives [15].

Sand blasting and laser shock processing both generate micro plastic deformation on the surface of materials, which results in compressive residual stress in the surface and near the surface regions, yielding good surface mechanical properties. Thin films deposition can also improve surface properties of Ti alloys, and protect materials from corrosion and friction wear. Improving the quality of coatings deposited on Ti alloys is an important research subject. Coatings deposition is one of the preferred methods to improve Ti alloys tribological properties. Pawlak et al. [16] deposited WC_{1-x}/C coatings on Ti-6Al-4V titanium alloy by reactive arc evaporation with the intermediate TiC_xN_y layer providing good adhesion and significantly increased wear resistance. Yonekura et al. studied arc ion plated Cr/CrN multilayer coatings with different number of layers on Ti-6Al-4V alloy substrates [17]. Ezazi et al. prepared Ti/TiN, Cr/CrN and TiCr/TiCrN thin film ceramic coatings on aerospace AL7075-T6 alloy, and significantly improved wear resistance and surface hardness of the substrate [18]. CrAlN ternary nitride has higher hardness, lower friction coefficient and higher thermal stability compared with CrN [19]. CrAlN coatings also have other excellent properties, such as hydrophobicity. Yang et al. deposited CrAlN films with improved performance, including higher contact angle and lower wear rate [20].

Changing the substrate temperature can affect the structure, residual stress and mechanical properties of the films [8]. Jeon et al. [21] studied the substrate temperature effects on residual stress in ZnO thin films prepared by ion beam deposition. Increasing the substrate temperature could shift the ZnO (002) reflection towards the ideal value, indicating the decrease of compressive residual stress in the films. The intermediate layer also plays an important role in the properties of the coatings [22,23]. Adhesion layer effects on wear properties of CrAlN coating have been studied, including Cr and TiN adhesion layers, and contributions to CrAlN coating mechanical properties had been considered [24–26]. The influence of atomic ratio of Cr and Al in CrAlN coatings was also investigated. It turns out that when x in the

* Corresponding author.
E-mail address: pangxl@mater.ustb.edu.cn (X. Pang).

https://doi.org/10.1016/j.ceramint.2017.12.037
Received 2 November 2017; Received in revised form 3 December 2017; Accepted 5 December 2017
Available online 06 December 2017

$Cr_{(1-x)}Al_xN$ films is between 0.6 and 0.7, the CrAlN coatings have better performance [27–29].

Also, residual stress in the thin films has a great influence on the full process of design, fabrication and package of the devices, and thus is an extremely important parameter in PVD coatings [30]. Huang et al. [31] explained that compressive stress was expected to blunt crack tips and inhibit crack propagation, while tensile stresses enlarged crack opening and facilitated crack propagation. Skordaris et al. [32] indicated that a certain residual stress level can be considered as optimal. B. Bouaouina studied the different bi-layer thickness effects on the residual stress, hardness and elastic modulus of the Mo_2N/CrN film [33]. Shot basting, laser beam heat treatment and ion implantation can generate compressive stress at the material surface, but these methods are not suitable for coating materials with the additional need of post-processing and raise the cost.

In this study, CrAlN coatings with different CrAl interlayer deposition temperatures were deposited on Ti alloys by radio frequency (RF) magnetron sputtering to investigate the effects of interlayer deposition temperature on residual stress, crystal structure and mechanical properties of the CrAlN coatings. A new method to deposit CrAlN coatings with relatively high residual stress without other pre- and post-processing is presented. This CrAlN deposition method provided a convenient and efficient way to deposit CrAlN coatings on Ti alloys with relatively high compressive residual stress and good mechanical properties.

2. Materials and experimental procedure

2.1. Film deposition

CrAlN films were deposited on two kinds of Ti-alloys substrates, TC4 and TC21, by RF magnetron sputtering, in order to serve as control experiments. Composition of the TC4 and TC21 alloys is listed in Table 1. It is known that Ti alloy is typically a fine-grained α + β alloy with approximately 20–30% primary α in a transformed β matrix, depending on the heat-treatment history [34–36]. The substrates dimensions were 20 mm × 10 mm × 3 mm. The surfaces were ground to 5000 grit and mechanically polished to mirror finish. Cr/Al alloy target with 3:7 Cr:Al atomic ratio was fixed in the cylindrical vacuum chamber. As shown in Fig. 1, the target was connected to the radio frequency power source and cooled by circulating water. The substrate was fixed on the sample holder at the top of the vacuum chamber. The holder was rotated during the deposition process to achieve uniform coating. A thermocouple was used to measure the substrate temperature during deposition. The vacuum chamber was grounded to achieve electrical neutrality of the system.

The base pressure was 5×10^{-3} Pa before the deposition process. CrAl interlayer was deposited prior to the CrAlN coating sputtering to improve its adhesion and control the coating residual stress by changing deposition temperature. CrAlN coating was deposited at 100 °C, while the CrAl interlayer deposition temperature was either 100 °C or 300 °C. The CrAlN deposition time was varied from 180 min to 300 min and the CrAl interlayer deposition time was 10 min.

Table 1
Composition of the TC4 and TC21 alloys.

Elements, wt%	Al	V	Fe	C	N	O	H	Ti
TC4	6.2	4.1	0.04	0.015	0.018	0.13	0.001	Balance

Elements, wt%	Al	Sn	Zr	Mo	Cr	Nb	Si	Fe	Ti
TC21	6–5.5	2	2	2.5–3	1.7	2	0.1	≦0.15	Balance

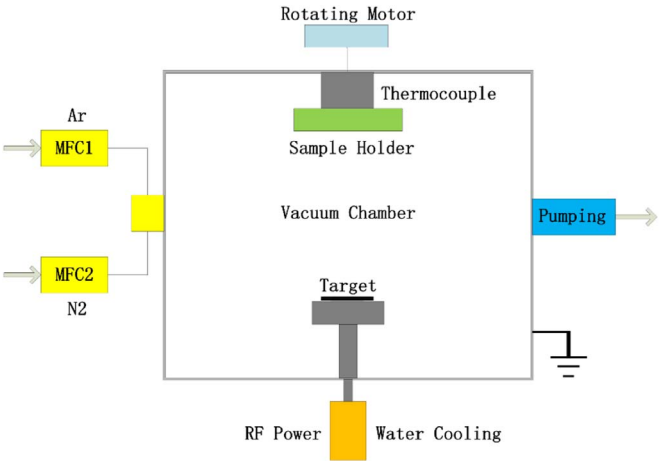

Fig. 1. Schematic diagram of the RF magnetron sputtering system.

2.2. Films characterization

The thickness of the coatings was measured by the white interference 3D microscopy (Bruker Nano GmbH, Bruker, Germany) and the cross section was observed by FESEM. Residual stress and the coating structure were characterized by X-ray diffraction (XRD) [37–40] using the Cu $K_{\alpha 1}$ line (0.15406 nm). The adhesion was measured by coating scratch test and the scratch track was observed by FESEM.

3. Results and discussion

3.1. Coating morphology and deposition rate

White interference 3D microscopy was used to obtain the coating thickness and surface morphology. Fig. 2**(a)** shows the surface morphology of the deposited coating, where the step in the middle of the image is represented by the coating red region and the substrate blue region. As seen in the coating red region, the film has good surface quality. Fig. 2**(b)** shows the line profile of the step, and ΔZ is the difference between the shadow regions, which represents the film thickness.

The thickness of CrAl interlayer is about 70 nm. The thickness of the coatings with the interlayer deposited at 100 °C and different CrAlN layer deposited for 180 min, 240 min, and 300 min is about 1.5 μm, 2 μm and 2.6 μm, respectively. Thus, the deposition rate of the CrAlN coatings is about 480 nm/h. The results were nearly the same for the films with the interlayer deposited at 300 °C. Fig. 3 shows cross-sectional micrographs of 2.6 μm CrAlN and 70 nm interlayer. The film structure is columnar with uniform grain size along with the cross section.

3.2. Crystal structure

Fig. 4 shows the crystal phase structure of the coatings of different thickness. The notation 300–100 means that the deposition temperatures of the interlayer and CrAlN coating was 300 °C and 100 °C, respectively, and 100-100 means that the deposition temperature of the interlayer and the CrAlN coating were both 100 °C. XRD patterns show preferred orientation of the CrAlN coatings with the interlayer deposited at different temperatures. The CrAlN film structure is based on the fcc-CrN structure, where the addition of Al in the form of solid solution has been shown to increase the high temperature oxidation resistance (700–800 °C) [41,42].

As shown in Fig. 4**(a),** when the interlayer deposition temperature was 300 °C, an obvious CrN (222) preferred orientation was observed and the (111) preferred orientation almost disappeared, compared with

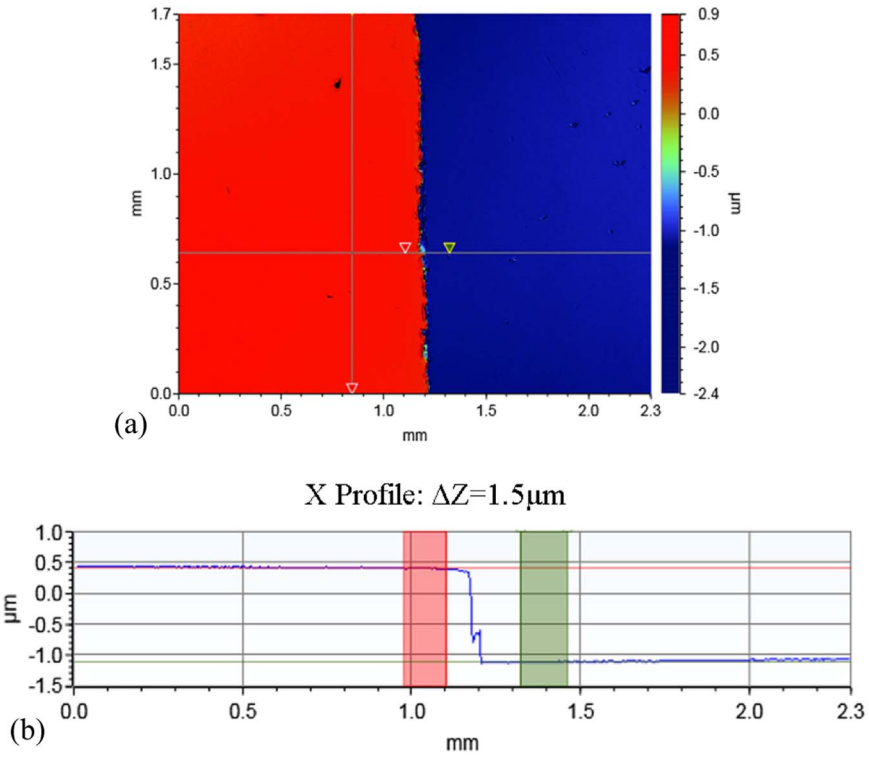

Fig. 2. Thickness measurements of the films by white interference 3D microscopy (300 °C adhesion layer deposition temperature, 180 min CrAlN layer deposition time and 100 °C temperature).

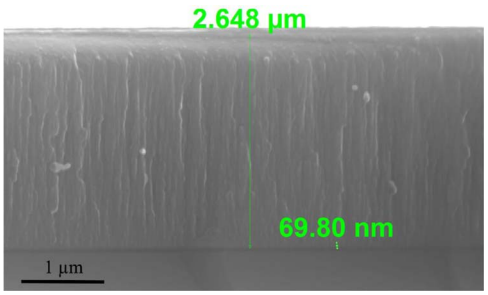

Fig. 3. FESEM cross-sectional micrographs of CrAlN coatings with deposition time 300 min.

the peaks deposited at 100 °C, for the 1.5 μm thick CrAlN coatings. The deposition parameters were same expect the interlayer deposition temperature, so the changes of preferred orientation were directly influenced by the interlayer deposition temperature. CrN (311) and (222) preferred orientation was observed when the coating thickness was 2 μm in Fig. 4**(b)**. The preferred orientation changed from CrN (111) and (222) to (220) and (222) as the film thickness increased to 2.5 μm in Fig. 4**(c)** when CrAl interlayer deposition temperature was increased from 100 °C to 300 °C.

The Bragg reflections corresponding to CrN indicated that the films were polycrystalline with random texture. Typical phase structure can be identified from the diffraction peaks CrN (111), CrN (220), CrN (311) and CrN (222). Ti_2N and TiN peaks come from the reaction of the Ti alloy substrate and N_2 gas at the initial film deposition stage. After the CrAl interlayer deposition, the substrate temperature decreased from 300 °C to 100 °C, and compressive stress occurred in the CrAl layer because of the substrate shrinkage, thus the strain energy was higher than the CrAl deposited at 100 °C. According to the theory of energy minimization [43], the total energy of coating depends on the strain energy and the surface energy. The close-packed (111) surface energy is the lowest, so preferred (111) orientation occurred in the CrAlN coatings with CrAl interayer deposited at 100 °C. The strain energy in the CrAl layer deposited at 300 °C is higher, so the preferred (111) orientation disappeared and turned into the orientation with lower strain energy.

The increase in various peaks intensity with thickness can be attributed to two factors [44], preferential orientation (texture development) of a particular plane and the increase in the volume of the diffracting material. When the film thickness increased, the initial increase of the CrN (311) peak intensity can be attributed to the higher diffraction volume, and the subsequent decrease in the (311) peak intensity can be attributed to the preferential orientation of the CrN (222) plane. At the same time, the CrN (222) preferred orientation decreased first and then increased as the film thickness increased, because of the influence of CrN (311).

3.3. Residual stress

Residual stress of the CrAlN coatings was analyzed using the Rigaku X-ray diffractometer (Smartlab), and calculations based on the $\sin^2 \Psi$ method, where Ψ is the angle between the normal to the coating surface and the diffracting lattice planes. The characteristic peak was CrN (220). The X-ray diffraction peak position shifts with the Ψ angle, and d_{hkl} has a linear relationship with $\sin^2\Psi$. The formula to calculate the residual stress is:

$$(d_{hkl} - d_0)/d_0 = \frac{1}{2}S_2 \bullet \sigma \bullet cos^2\,\alpha \bullet sin^2\,\Psi + \frac{1}{2}S_2 \bullet \sigma \bullet sin^2\,\alpha + 2S_1 \bullet \alpha \quad (1)$$

Here, S_2 and S_1 are coating constants related to the Poisson's ratio (approximately equal to 0.3) and elastic modulus (determined by nanoindentation, different for the coatings with different thickness, but approximately equal to 155 GPa). α is the angle related to the 2θ diffraction angle and Ψ = 0°, 15°, 20°, 25°, 30°, 35°, 40° and 45°. The CrN (220) peak positions at different Ψ are shown in Fig. 5. The calculated residual stress results are shown Fig. 6. Here, the 100-100 TC4 notation means that the deposition temperature for the CrAl interlayer and the CrAlN coating are both 100 °C, while the substrate material is TC4. Other data are named using the same notation.

All measured residual stresses are negative, i.e. compressive, which is beneficial for the coating mechanical performance. Residual stress in

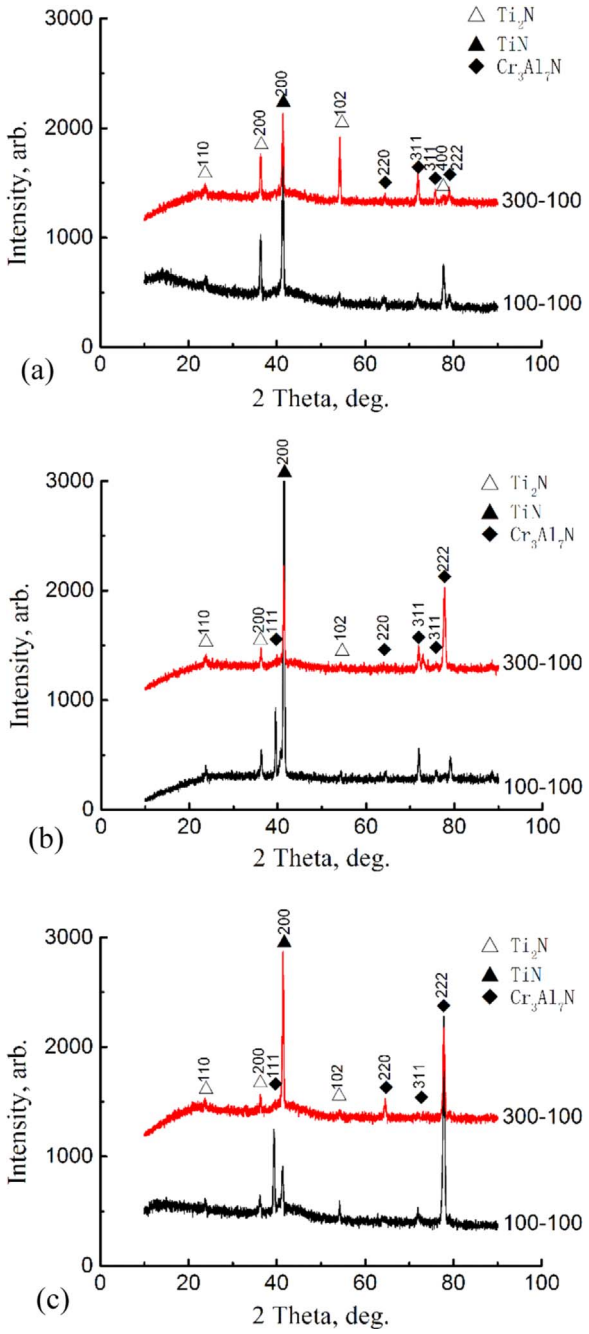

Fig. 4. XRD patterns of CrAlN coatings with different thickness: (a) 1.5 μm, (b) 2 μm and (c) 2.6 μm.

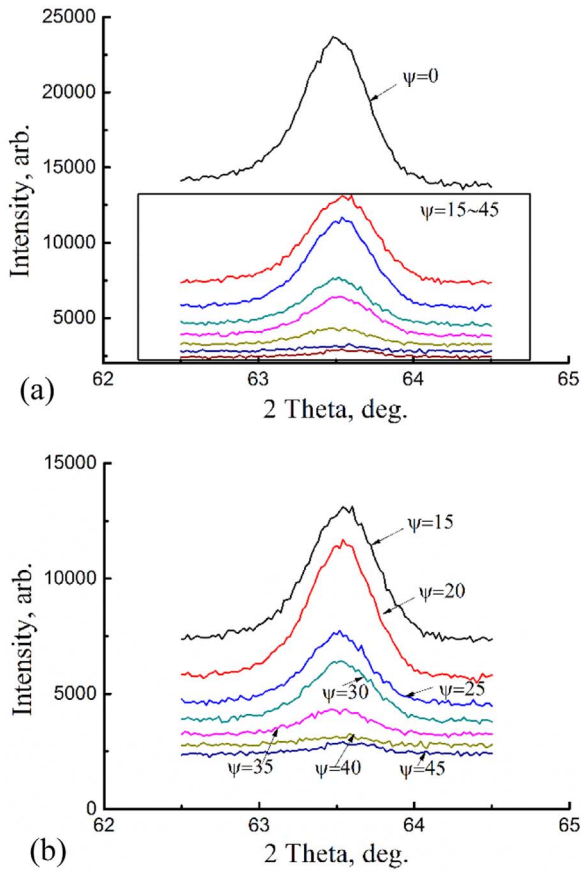

Fig. 5. CrN (220) reflections at different Ψ angles (a) and magnified area (b).

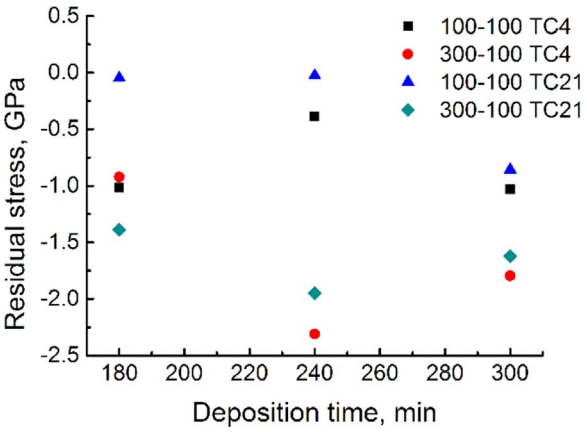

Fig. 6. Residual stress in CrAlN coatings with different deposition time and interlayer deposition temperature. (300–100 means 300 °C CrAl interayer deposition temperature and 100 °C CrAlN coating deposition temperature, and other notation express the same way.).

1.5 μm, 2 μm and 2.6 μm thick CrAlN films on TC21 with the interlayer deposited at 100 °C was −47.43 MPa, −25.57 MPa and −855.77 MPa, respectively. For the interlayer deposited at 300 °C the residual stress was −1.39 GPa, −1.95 GPa and −1.62 GPa, respectively. The coatings' residual stress on the TC4 substrate was −1.02 GPa, −389.91 MPa and −1.03 GPa for the interlayer deposited at 100 °C, respectively, and −921.42 MPa, −2.31 GPa and −1.8 GPa for the interlayer deposited at 300 °C, respectively. It's clear that when the deposition temperature of the CrAl interlayer is 300 °C, the residual stress in the CrAlN coatings is much higher compared with the CrAl interlayer deposited at 100 °C. All deposition parameters were fixed, except for the adhesion layer deposition temperature. Summing up the above discussion, changing the interlayer deposition temperature influenced the microstructure of the coatings, as the residual stress changed at the same time.

3.4. Coating scratch test

Scratch tests were performed using the UMT Tribometer with Si_3N_4 ball with 20 μm radius tip. The load-friction curve is shown in Fig. 7**(a)**. The coating failure process can be divided into three stages. (1) The load was relatively small, and the friction changed a little. When the coating's strength was higher than the indenter pressure, there were tiny cracks. (2) The load increased, and the friction changed severely. Cracks appeared until the coating completely failed. This stage started

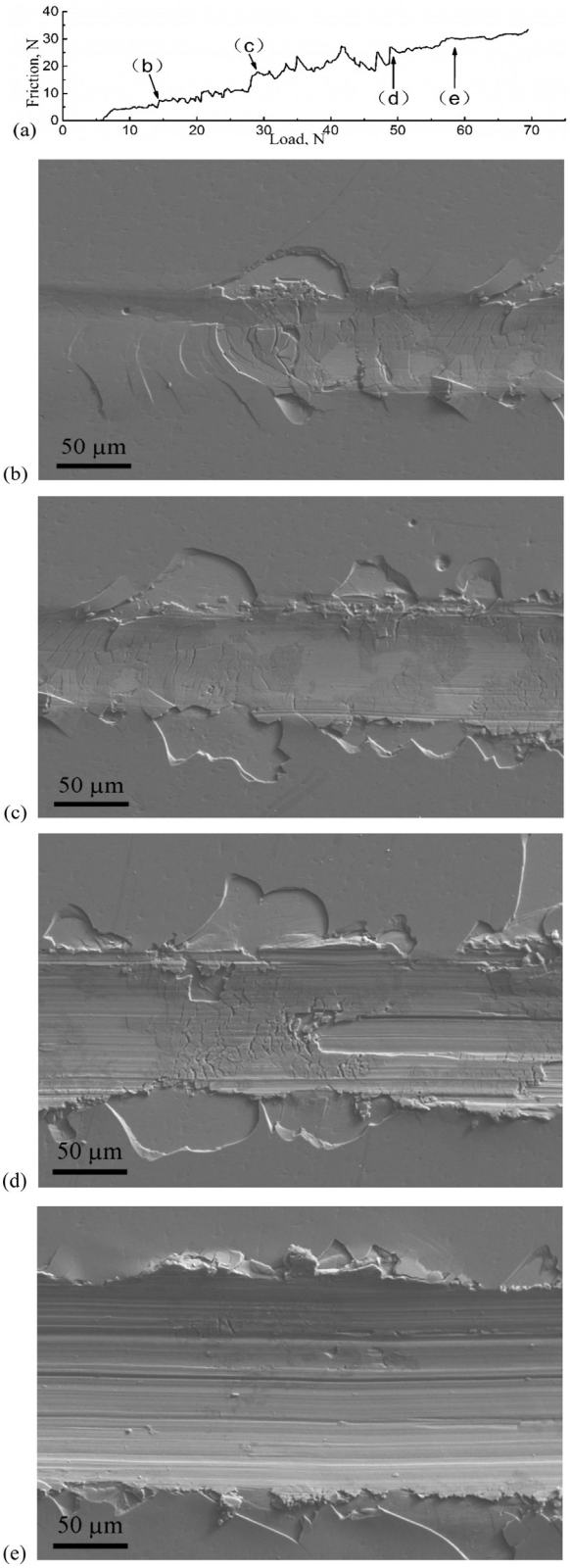

Fig. 7. Scratch morphology (b)(c)(d)(e) and friction-load curve (a) of scratch test on CrAlN coating, TC4 substrate, CrAl layer deposition temperature 100 °C, CrAlN coating thickness 2.6 μm.

once the first crack appeared, starting the coating failure. (3) The load increased to a much higher value, but the friction remained stable. The coating failed completely, and the indenter scratched on the substrate directly, so friction changed a little. The load generating the first crack

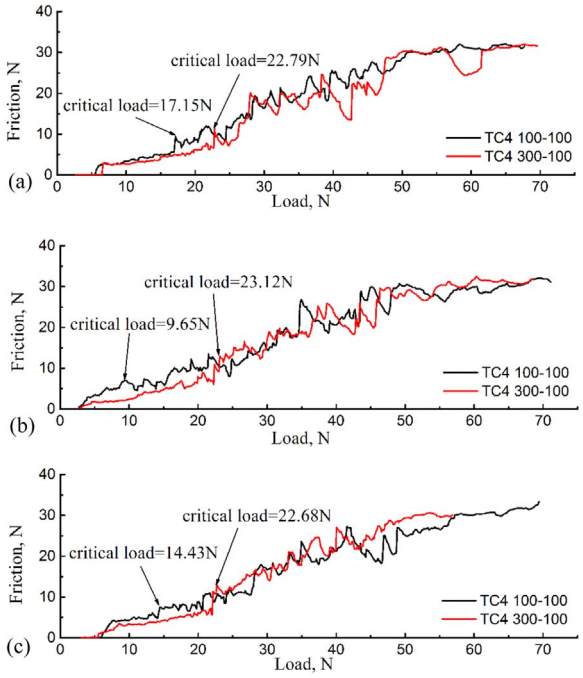

Fig. 8. Friction-load curves of scratch test on CrAlN coatings, film thickness (a) 1.5 μm, (b) 2 μm and (c) 2.6 μm.

(film crack initiation point) is related to strength and adhesion of the coatings. Higher load means better adhesion and coating strength.

Fig. 8 shows the friction-load curves of the scratch test performed on the CrAlN coatings deposited on the TC4 substrate with different CrAlN coating deposition time and CrAl layer deposition temperature. The critical load for film crack initiation is 17.15 N, 9.65 N and 14.43 N for 100 °C CrAl layer deposition temperature and CrAlN film thickness of 1.5 μm, 2 μm and 2.6 μm, respectively. The corresponding critical load for the 300 °C CrAl layer deposition temperature is 22.79 N, 23.12 N and 22.68 N, respectively. These results showed that the CrAlN coatings with the CrAl layer deposited at 300 °C had higher strength and adhesion than at 100 °C. Although the critical load can be affected by both internal stress and formation of interfacial mixing layer, the residual stress of the coatings plays a major role. The higher critical load results can be regarded as the effects of the increasing residual stress in the CrAlN coatings.

Fig. 9 shows the scratch morphology of the CrAlN coatings on the TC4 substrate during stage 2 failure. Failure modes of the CrAlN coatings with different CrAl interlayer deposition temperature were different. There were many tiny cracks along the coating scratch for the coatings with 300 °C CrAl layer deposition temperature, the failure mode was film cracking under high applied loading. While the morphology of scratch on the coatings with 100 °C CrAl layer deposition temperature were featured by flaking, induced by relatively poor adhesion strength. The results declared that the higher adhesion layer deposition temperature, also led to better adhesion strength of the coatings.

4. Conclusions

In this study, CrAlN coatings with CrAl interlayer deposited at 100 °C and 300 °C, were prepared on TC4 and TC21 alloys using RF magnetron sputtering. Changing the interlayer deposition temperature significantly influenced residual stress and crystal structure of the coatings. Residual stress in the CrAlN coatings was compressive. The CrAlN coatings with interlayer deposited at 300 °C had higher residual stress than at 100 °C.

Compressive residual stress differences between the coatings with

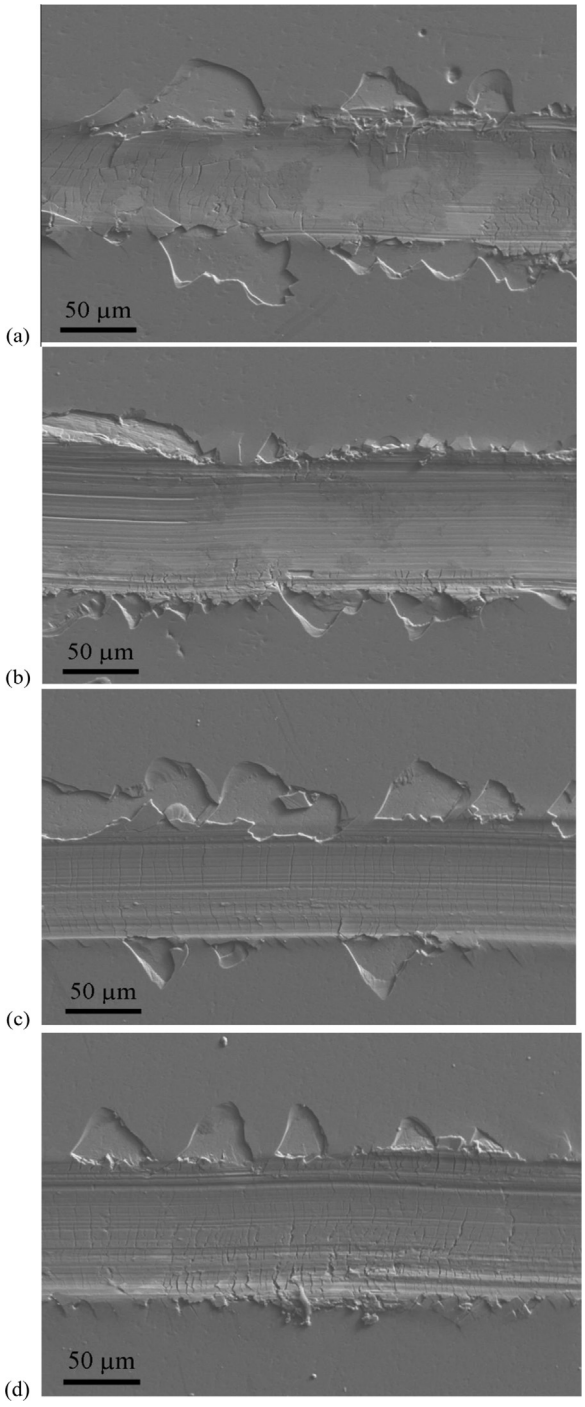

Fig. 9. Scratch morphology of CrAlN coatings on TC4 substrate, CrAl deposition temperature (a) (b) 100 °C and (c) (d) 300 °C, CrAlN thickness 2.6 μm.

adhesion layer deposition temperature of 300 °C and 100 °C for different film thickness (1.5 μm, 2.0 μm, 2.5 μm) are about 1.34 GPa, 1.92 GPa and 766.38 MPa, respectively. Thus, not only the film thickness can influence the internal stress of the substrate surface, but also the adhesion layer deposition temperature. The adhesion layer deposition temperature can significantly influence the CrAlN crystallization. The preferred orientation of the CrAlN coatings changed from CrN (111) to CrN (222) when interlayer deposition temperature was increased to 300 °C. The coating scratch test results show that the adhesion and coating strength of coatings with higher residual stress was higher.

Acknowledgements

This work was supported by the Beijing Nova Program (Z171100001117075), the National Natural Science Foundation of China (51771025) and the Fundamental Research Funds for the Central Universities (FRF-TP-17-002C1).

References

[1] J.H. Zuo, Z.G. Wang, E.H. Han, Effect of microstructure on ultra-high cycle fatigue behavior of Ti–6Al–4V, Mater. Sci. Eng.: A 473 (2008) 147–152.
[2] N. Verdhan, D.D. Bhende, R. Kapoor, J.K. Chakravartty, Effect of microstructure on the fatigue crack growth behaviour of a near-α Ti alloy, Int. J. Fatigue 74 (2015) 46–54.
[3] I. Bantounas, T.C. Lindley, D. Rugg, D. Dye, Effect of microtexture on fatigue cracking in Ti–6Al–4V, Acta Mater. 55 (2007) 5655–5665.
[4] D. Cressman, B. Tury, G.L. Doll, Effects of surface treatments and coatings on tribological performance of Ti–6Al–4V in the mixed fretting and gross slip regimes, Surf. Coat. Technol. 276 (2015) 260–265.
[5] J. Ding, G. Bandak, S.B. Leen, E.J. Williams, P.H. Shipway, Experimental characterisation and numerical simulation of contact evolution effect on fretting crack nucleation for Ti–6Al–4V, Tribol. Int. 42 (2009) 1651–1662.
[6] L. Jin, A.R. Riahi, K. Farokhzadeh, A. Edrisy, Investigation on interfacial adhesion of Ti–6Al–4V/nitride coatings, Surf. Coat. Technol. 260 (2014) 155–167.
[7] C.M. Lee, J.P. Chu, W.Z. Chang, J.W. Lee, J.S.C. Jang, P.K. Liaw, Fatigue property improvements of Ti–6Al–4V by thin film coatings of metallic glass and TiN: a comparison study, Thin Solid Films 561 (2014) 33–37.
[8] G. Liu, Y. Yang, B. Huang, X. Luo, S. Ouyang, G. Zhao, et al., Effects of substrate temperature on the structure, residual stress and nanohardness of Ti6Al4V films prepared by magnetron sputtering, Appl. Surf. Sci. 370 (2016) 53–58.
[9] J.C. Avelar-Batista Wilson, S. Wu, I. Gotman, J. Housden, E.Y. Gutmanas, Duplex coatings with enhanced adhesion to Ti alloy substrate prepared by powder immersion nitriding and TiN/Ti multilayer deposition, Mater. Lett. 157 (2015) 45–49.
[10] T. Sprute, W. Tillmann, D. Grisales, U. Selvadurai, G. Fischer, Influence of substrate pre-treatments on residual stresses and tribo-mechanical properties of TiAlN-based PVD coatings, Surf. Coat. Technol. 260 (2014) 369–379.
[11] W. Tillmann, E. Vogli, S. Momeni, Improvement of press dies used for the production of diamond composites by means of DUPLEX-PVD-coatings, Surf. Coat. Technol. 205 (2010) 1571–1577.
[12] F.F. Komarov, V.M. Konstantinov, A.V. Kovalchuk, S.V. Konstantinov, H.A. Tkachenko, The effect of steel substrate pre-hardening on structural, mechanical, and tribological properties of magnetron sputtered TiN and TiAlN coatings, Wear 352–353 (2016) 92–101.
[13] J.C.A. Batista, C. Godoy, V.T.L. Buono, A. Matthews, Characterisation of duplex and non-duplex (Ti, Al)N and Cr–N PVD coatings, Mater. Sci. Eng.: A 336 (2002) 39–51.
[14] K. Farokhzadeh, A. Edrisy, Fatigue improvement in low temperature plasma nitrided Ti–6Al–4V alloy, Mater. Sci. Eng.: A 620 (2015) 435–444.
[15] D. Fan, X. Liu, J. Huang, R. Fu, S. Chen, X. Zhao, An ultra-hard and thick composite coating metallurgically bonded to Ti–6Al–4V, Surf. Coat. Technol. 278 (2015) 157–162.
[16] W. Pawlak, K.J. Kubiak, B.G. Wendler, T.G. Mathia, Wear resistant multilayer nanocomposite WC1 − x/C coating on Ti–6Al–4V titanium alloy, Tribol. Int. 82 (2015) 400–406.
[17] D. Yonekura, J. Fujita, K. Miki, Fatigue and wear properties of Ti–6Al–4V alloy with Cr/CrN multilayer coating, Surf. Coat. Technol. 275 (2015) 232–238.
[18] M.A. Ezazi, M.M. Quazi, E. Zalnezhad, A.A.D. Sarhan, Enhancing the tribo-mechanical properties of aerospace AL7075-T6 by magnetron-sputtered Ti/tin, Cr/CrN & TiCr/TiCrN thin film ceramic coatings, Ceram. Int. 40 (2014) 15603–15615.
[19] C. Yu, S. Wang, L. Tian, T. Li, B. Xu, Microstructure and mechanical properties of CrAlN coatings deposited by modified ion beam enhanced magnetron sputtering on AISI H13 steel, J. Mater. Sci. 44 (2008) 300–305.
[20] Y.-S. Yang, T.-P. Cho, J.-H. Lin, Optimizing hydrophobic and wear-resistant properties of Cr–Al–N coatings, Thin Solid Films 544 (2013) 612–616.
[21] J.-W. Jeon, M. Kim, L.-W. Jang, J.L. Hoffman, N.S. Kim, I.-H. Lee, Effect of substrate temperature on residual stress of ZnO thin films prepared by ion beam deposition, Electron. Mater. Lett. 8 (2012) 27–32.
[22] J.-H. Zheng, M. Kato, K. Nakasa, Effect of intermediate layer on wear-delamination life of low-frictional SiC-2.6mass%Ti film sputter-deposited on titanium substrate, Surf. Coat. Technol. 205 (2010) 2532–2537.
[23] L. Wan, G. Thompson, Influence of Fe underlayers on stress evolution of Ti in Ti/Fe multilayers, J. Vac. Sci. Technol. A: Vac. Surf. Films 34 (2016) 061501.
[24] Q. Wang, F. Zhou, J. Yan, Evaluating mechanical properties and crack resistance of CrN, CrTiN, CrAlN and CrTiAlN coatings by nanoindentation and scratch tests, Surf. Coat. Technol. 285 (2016) 203–213.
[25] N.E. Beliardouh, K. Bouzid, C. Nouveau, B. Tlili, M.J. Walock, Tribological and electrochemical performances of Cr/CrN and Cr/CrN/CrAlN multilayer coatings deposited by RF magnetron sputtering, Tribol. Int. 82 (2015) 443–452.
[26] M. Okumiya, M. Griepentrog, Mechanical properties and tribological behavior of tin–CrAlN and CrN–CrAlN multilayer coatings, Surf. Coat. Technol. 112 (1999) 123–128.
[27] H. Makoto, U. Yasuhiro, S. Tsuneo, J. Weihua, G. Constantin, Y. Kiyoshi, Characteristics of (Cr 1- x, Al x)N films prepared by pulsed laser deposition, Jpn. J. Appl. Phys. 40 (2001) 1056.

[28] A.E. Reiter, V.H. Derflinger, B. Hanselmann, T. Bachmann, B. Sartory, Investigation of the properties of Al1 − xCrxN coatings prepared by cathodic arc evaporation, Surf. Coat. Technol. 200 (2005) 2114–2122.
[29] O. Banakh, P.E. Schmid, R. Sanjinés, F. Lévy, High-temperature oxidation resistance of Cr1 − xAlxN thin films deposited by reactive magnetron sputtering, Surf. Coat. Technol. 163–164 (2003) 57–61.
[30] F. Vaz, L. Rebouta, P. Goudeau, J.P. Rivière, E. Schäffer, G. Kleer, et al., Residual stress states in sputtered Ti1 − xSixNy films, Thin Solid Films 402 (2002) 195–202.
[31] Y.-C. Huang, S.-Y. Chang, C.-H. Chang, Effect of residual stresses on mechanical properties and interface adhesion strength of SiN thin films, Thin Solid Films 517 (2009) 4857–4861.
[32] G. Skordaris, K.D. Bouzakis, T. Kotsanis, P. Charalampous, E. Bouzakis, B. Breidenstein, et al., Effect of PVD film's residual stresses on their mechanical properties, brittleness, adhesion and cutting performance of coated tools, CIRP J. Manuf. Sci. Technol. 18 (2017) 145–151.
[33] B. Bouaouina, A. Besnard, S.E. Abaidia, F. Haid, Residual stress, mechanical and microstructure properties of multilayer Mo_2N/CrN coating produced by R.F magnetron discharge, Appl. Surf. Sci. (2016).
[34] N. Poondla, T.S. Srivatsan, A. Patnaik, M. Petraroli, A study of the microstructure and hardness of two titanium alloys: commercially pure and Ti–6Al–4V, J. Alloy. Compd. 486 (2009) 162–167.
[35] I. Bantounas, D. Dye, T.C. Lindley, The role of microtexture on the faceted fracture morphology in Ti–6Al–4V subjected to high-cycle fatigue, Acta Mater. 58 (2010) 3908–3918.
[36] J.H. Luan, Z.B. Jiao, W.H. Liu, Z.P. Lu, W.X. Zhao, C.T. Liu, Compositional and microstructural optimization and mechanical-property enhancement of cast Ti alloys based on Ti-6Al-4V alloy, Mater. Sci. Eng.: A 704 (2017) 91–101.
[37] E. Bemporad, M. Brisotto, L.E. Depero, M. Gelfi, A.M. Korsunsky, A.J.G. Lunt, et al., A critical comparison between XRD and FIB residual stress measurement techniques in thin films, Thin Solid Films 572 (2014) 224–231.
[38] S. Chowdhury, M.T. Laugier, J. Henry, XRD stress analysis of CVD diamond coatings on SiC substrates, Int. J. Refract. Metals Hard Mater. 25 (2007) 39–45.
[39] E. Mohammadpour, Z.-T. Jiang, M. Altarawneh, Z. Xie, Z.-f. Zhou, N. Mondinos, et al., Predicting high temperature mechanical properties of CrN and CrAlN coatings from in-situ synchrotron radiation X-ray diffraction, Thin Solid Films 599 (2016) 98–103.
[40] T. Teppernegg, P. Angerer, T. Klünsner, C. Tritremmel, C. Czettl, Evolution of residual stress in Ti–Al–Ta–N coatings on hard metal milling inserts, Int. J. Refract. Metals Hard Mater. 52 (2015) 171–175.
[41] H.C. Barshilia, N. Selvakumar, B. Deepthi, K.S. Rajam, A comparative study of reactive direct current magnetron sputtered CrAlN and CrN coatings, Surf. Coat. Technol. 201 (2006) 2193–2201.
[42] Y. Lv, L. Ji, X. Liu, H. Li, H. Zhou, J. Chen, The structure and properties of CrAlN films deposited by mid-frequency unbalanced magnetron sputtering at different substrate bias duty cycles, Surf. Coat. Technol. 206 (2012) 3961–3969.
[43] D.N. Lee, A model for development of orientation of vapour deposits, J. Mater. Sci. 24 (1989) 4375–4378.
[44] T. Prasanna Kumari, M. Manivel Raja, A. Kumar, S. Srinath, S.V. Kamat, Effect of thickness on structure, microstructure, residual stress and soft magnetic properties of DC sputtered Fe65Co35 soft magnetic thin films, J. Magn. Magn. Mater. 365 (2014) 93–99.